DOI: 10.1002/ ((please add manuscript number))

Article type: Full Paper

3D Electrophoresis-Assisted Lithography (3DEAL): 3D molecular printing to create functional patterns and anisotropic hydrogels

*Juan P. Aguilar, Michal Lipka, Gastón A. Primo, Edxon E. Licon-Bernal, Juan M. Fernández-Pradas, Andriy Yaroshchuk, Fernando Albericio, Alvaro Mata**

J. P. Aguilar, Prof. A. Mata
The Nanotechnology Platform
Parc Científic Barcelona,
08028, Spain.
Email: a.mata@qmul.ac.uk

J. P. Aguilar, Prof. F. Alberico
Institute for Research in Biomedicine,
Baldiri Reixac 10–12,
08028, Spain.

J. P. Aguilar
Tecnologico de Monterrey, Campus Guadalajara
Av. General Ramón Corona 2514, Zapopan, Jal
45138, México.

M. Lipka, G. A. Primo, Prof. A. Mata
School of Engineering and Materials Science,
Queen Mary University of London, Mile End Road,
E14NS, UK.
Email: a.mata@qmul.ac.uk

G. A. Primo, Prof. A. Mata
Institute of Bioengineering,
Queen Mary University of London, Mile End Road,
E14NS, UK.
Email: a.mata@qmul.ac.uk

E. E. Licon-Bernal, Dr. A. Yaroshchuk
Department of Chemical Engineering,
Polytechnic University of Catalonia, Diagonal 647,
08028, Spain.

Dr. J. M. Fernández-Prada
Departament de Física Aplicada i Òptica, Martí i Franquès 1,
Universitat de Barcelona,
08028, Spain.

Dr. A. Yaroshchuk
Institution for Research and Advanced Studies (ICREA),
Passeig Lluís Companys 23,
08010, Spain.

Prof. F. Alberico
CIBER-BBN, Networking Centre on Bioengineering, Biomaterials and Nanomedicine,
Department of Organic Chemistry, University of Barcelona,
08028, Spain.

Prof. F. Alberico
School of Chemistry & Physics,
University of KwaZulu-Natal, 4001-Durban,
4041, South Africa.

Keywords: 3D patterning, molecular printing, electrophoresis, lithography, anisotropic hydrogels

The ability to easily generate anisotropic hydrogel environments made from functional molecules with microscale resolution is an exciting possibility for the biomaterials community. This study reports a novel 3D-Electrophoresis-Assisted-Lithogrpahy (3DEAL) platform that combines elements from proteomics, biotechnology, and microfabrication to print well-defined 3D molecular patterns within hydrogels. The potential of the 3DEAL platform is assessed by patterning immunoglobulin G, fibronectin, and elastin within nine widely used hydrogels and characterizing pattern depth, resolution, and aspect ratio. Furthermore, the technique's versatility is demonstrated by fabricating complex patterns including parallel and perpendicular columns, curved lines, gradients of molecular composition, and patterns of multiple proteins ranging from tens of microns to centimeters in size and depth. The functionality of the printed molecules is assessed by culturing NIH-3T3 cells on a fibronectin-patterned polyacrylamide-collagen hydrogel and selectively supporting cell growth. 3DEAL is a simple, accessible, and versatile hydrogel-patterning platform based on controlled molecular printing that may enable the development of tunable, chemically anisotropic, and hierarchical 3D environments.

1. Introduction

There is growing and widespread interest in the fabrication of complex and tunable environments for a variety of applications. For example, within the field of tissue engineering, hydrogel scaffolds are increasingly exhibiting structural and functional elements that mimic the natural extracellular matrix (ECM).[1] These materials are being developed for *in vivo* applications as intelligent matrices able to recruit, support, and guide cell growth for tissue regeneration,[2] control biological processes,[3] or deliver bioactive molecules.[4] Other hydrogel systems are also enabling the development of scaffolds to be used as 3D *in vitro* culture systems for improved cell studies,[5] drug discovery,[6] embryology,[7] and tissue engineering.[8] Other examples can be found in the bio-catalytic,[9] biochemical,[10] and biopharmaceutical[11] fields where the need for a controlled spatial distribution of molecules, viruses, or micro-organisms is growing. However, there is still limited capacity to create complex 3D environments that provide controlled biochemical anisotropy through the spatial control of structural and functional molecules such as peptides, proteins, or glycans.

The opportunities emerging from spatially controlling biochemical composition and functionality have been enormous in biological and biomedical applications. The last two decades have seen a rapid increase in the development of two-dimensional (2D) surfaces with precise molecular patterns (e.g. cell adhesive ligands) using techniques such as soft lithography,[12] dip pen nanolithography,[13] photolithography,[14] nanoimprint lithography,[15] and microfluidic devices.[16] However, these surfaces are not an adequate representation of the natural 3D cellular environment, which significantly limits their

effectiveness and functionality.[17] Therefore, there is great need to develop hydrogel materials that are capable of exhibiting the molecular anisotropy and complexity of such 2D molecular patterns, but within more biomimetic 3D environments.[18] Towards this goal, a number of research groups are developing a wide variety of fabrication approaches ranging from traditional techniques based on microfluidics[19] or stereolithography[20] to more complex systems such as bioprinting multilayered structures,[21] additive photopatterning,[22,23] 3D printing,[24] directed self-assembly,[25-27] and sequential click reactions with photoaddition.[28,29] While these strategies enable anisotropic 3D environments with molecular patterns, they still have disadvantages such as the need for hydrogels that are specifically designed for the particular patterning technique, the use of potentially harmful UV radiation, limited capacity to pattern large or complex molecules such as functional proteins or drugs, and a requirement for sophisticated equipment, chemical reactions, and expensive processes.

Recently, there has been interest in the use of electrical fields (EFs) for 3D patterning. This method controls the motion of dispersed charged particles through an EF using either direct[30-32] or alternating[33,34] current. The use of direct current to move any kind of charged molecule in a uniform EF is termed electrophoresis. This electrokinetic process involves the presence of electrodes to apply the EF and an appropriate buffer solution made from a mixture of ions in order to facilitate the current in combination with an optimum pH. The use of electrophoresis as a tool to manipulate charged molecules represents a simple and affordable strategy to guide their localization within hydrated 3D environments with biological relevance.

Here, we report a novel 3D-Electrophoresis-Assisted-Lithogrpahy (3DEAL) platform to create molecular patterns within 3D hydrogel materials. The technique integrates fundamental principles from native polyacrylamide gel electrophoresis (NPAGE) by using EFs to manipulate proteins in their native state; affinity chromatography by immobilizing molecules within a hydrogel; and microfabrication by using a porous mask to define the printing regions. The resulting 3DEAL is a simple, affordable, tunable, and versatile technique that enables the creation of 3D anisotropic and hierarchical hydrogel environments exhibiting functional patterns.

2. Results and Discussion

2.1. 3DEAL Components

The 3DEAL platform uses electrophoresis to move functional molecules in their native state, independently of their charge and size, and precisely localize them within hydrogels. The technique comprises five simple components including a power supply, two platinum electrodes (connected to the power supply), two containers that enclose the buffer solution, a capsule containing the hydrogel, and tubing connecting the capsule to the buffer containers **(Figure 1a and b)**. The capsule holds together the hydrogel and the mask **(Figure 1c)**. Three slightly different configurations of the capsule (basic, glass, and poly methyl methacrylate (PMMA)) were developed in order to facilitate filling of the hydrogel and printing solution and experimental visualization **(Figure 1d-g and S1)**. The basic capsule fabricated from the Eppendorf and flat bottom tubes is inexpensive, disposable, and enables generation of well-defined patterns within a high volume of hydrogel in a single

process **(Figure S1a)**. The glass capsule facilitates visualization and characterization of the patterning process **(Figure S1b)**. The PMMA capsule allows better control over the assembly of the device and the possibility of using small volume hydrogels as well as patterning hydrogels with low stiffness **(Figure S1c)**. All configurations were designed to focus the EF and facilitate the migration of water molecules, ions from the buffer solution, and printing molecules through the hydrogels **(Figure 1c)**. The setup also results in low power consumption, which opens the possibility to connect several capsules in parallel and reduce printing time **(Figure S2)**. Platinum electrodes were selected because of their inertness and low degradation rate, while Tris-HCl and Tris-Glycine were chosen as buffer solutions to maintain a constant pH and temperature (21 °C) during the patterning process. The mask, a porous membrane with precise through-holes, defines the regions where printing takes place and, as described below, is a major design element and plays a key role on the tuneability and performance of the 3DEAL process.

2.2. 3DEAL Process

The 3DEAL process uses electrophoresis to drag the printing molecules along the direction of the EF. Together with the mask, the EF directs the migration of these molecules suspended in the printing solution towards the electrode of opposite charge **(Figure 1c)**. Critical to the patterning process is the capacity to enable the movement of ions from the buffer solution and water molecules across the mask to minimize the changes of the electric field across the printing solution-mask-hydrogel interfaces. Upon application of the EF, the printing molecules migrate towards the mask, across which water molecules and ions from the buffer are able to pass through the mask due to their smaller size compared to the pores

within the structure of the mask, but the larger printing molecules are only able to pass through the mask through-holes **(Figure 1c and 2b)**. In this way, the molecules are precisely focused via the mask through-holes and printed within the hydrogel as defined by the EF.

2.3. Mask Permeability

A critical design element of the 3DEAL platform is the use of a mask with optimum porosity and permeability. The mask, made from a commercially available dialysis membrane (Spectra/Por® 7, Spectrum®Lab., USA), must be permeable to ions from the buffer and water molecules but impermeable to the printing molecules **(Supporting Section 4)**. In this study, we refer to "mask through-holes" the holes that are fabricated on the mask and used to define the patterning regions within the hydrogels, and "mask porosity" the inherent pores that are present in the mask material. Inappropriate permeability disrupts the EF and the efficiency of the electrophoresis effect, resulting in poorly controlled and distorted patterns.

To optimize the mask permeability, numerical simulations were conducted **(Figure 2c)**. The model comprised a mask with a single through-hole that connected two different domains, which corresponded to two locations on each side of the mask. One domain is the hydrogel to be patterned while the other corresponds to the solution with the printing molecule prior to the patterning process, which was designed to have a porosity distribution similar to that of the hydrogel **(Figure 2a-c)**. The behaviour of the EF and the

electrophoresis effect were described by different governing equations **(Equation S1-10)**, which included a velocity component of the flux of the printing molecules through the hydrogel that estimates the displacement of these molecules. Using a model for an impermeable mask, the simulations revealed a large velocity gradient with printing molecules moving slower in closer proximity to the mask and faster as they get further from it, clearly affecting the directionality of the EF **(Figure 2c2)**. Increasing the average permeability of the mask resulted in a more directionally consistent EF **(Figure 2c3)**. However, the efficiency of the electrophoresis effect remains low and, as a consequence, produces abrupt velocity changes in the migration of the ions from the buffer, water molecules, and printing molecules. These velocity gradients provoke a significant enlargement and distortion of the molecular patterns compared to the geometry defined by the through-hole of the mask **(Figure 2c2 and c3)**. Finally, the numerical simulations predicted that in order to maximize agreement between the size and geometry of the mask through-holes and the corresponding molecular patterns in the hydrogel, the mask structure should have sufficiently large pores (porosity). In this way, the ions from the buffer and water molecules are able to move through the mask, enabled by the inherent porosity of its structure, while the printing molecules would only be able to cross the mask via its fabricated through-holes **(Figure 2b)**. Thus, the velocity gradients are avoided, increasing efficiency of the electrophoresis effect, and improving control of the printing direction **(Figure 2c4)**.

To validate the results from the simulations, we fabricated an impermeable mask using polydimethylsiloxane (PDMS) and two semi-permeable masks using dialysis membranes

with two distinct molecular weight cut-off (MWCO) values (3.5 kDa MWCO and 50 kDa MWCO) below the molecular weight of the printing protein (175 kDa). Polyacrylamide-Gelatin Type A (PA-GelA) composite was used as the hydrogel to be patterned and blue fluorescently-labeled immunoglobulin G (bIgG) was used as the printing molecule. In accordance to the numerical simulations described above, running of the 3DEAL process using the PDMS mask resulted in significantly enlarged patterns **(Figure 2d2)**. In contrast, running of the 3DEAL with the lowest MWCO mask generated significantly narrower patterns but still exhibited considerable enlargement **(Figure 2d3)**. Further increasing the permeability of the mask resulted in much narrower patterns that more closely resemble the dimensions and geometry of the mask through-holes **(Figure 2d4)**. As demonstrated by the simulations, this mask was able to prevent the passage of the printing molecules but enabled, with more freedom, the movement of ions, resulting in more homogenous migration velocities of the printing molecules and subsequently a better defined pattern. This behaviour was observed using masks with other MWCOs and independently of the diameter of the through-holes **(Figure S2a-c)**. These results demonstrate the possibility to control the resolution of the 3DEAL technique by simply adjusting the MWCO of the mask according to the molecular weight of the printing molecule.

2.4. Process Performance and Versatility

Using a 50 kDa MWCO mask, bIgG (150 kDa MW) patterns of 150 µm in diameter and 5 mm in depth were printed within a PA-GelA **(Figure 3a and b)**. The pattern geometry is preserved within and throughout the hydrogel with respect to the size and geometry of the mask through-holes. In some hydrogels such as PA and PA-GelA, a minor pattern

distortion is observed in close proximity to the mask, primarily due to a distortion of the hydrogel as a consequence of the capsule used **(Figure 3b)**. To demonstrate the versatility and potential broad applicability of the 3DEAL platform, we evaluated the technique using a variety of hydrogel materials and printing molecules including bIgG, green fluorescently-labeled immunoglobulin G (gIgG), elastin, and fibronectin (FN). The proteins gIgG and bIgG were used to characterize in more detail the patterning process within nine readily available hydrogels with distinct properties in terms of their suitability to be used for cell culture[1-4] **(Figure 3)**. Arrays of 200 μm diameter and 5 mm deep column-patterns were printed using specific processing time, voltage, and protein concentration in the printing solution. The quality of the patterning process was characterized by measuring the difference between the area of the printed region (pr) and the through-hole diameter (hd) of the mask **(Figure 3)**. Immunofluorescence imaging demonstrated that patterns were printed within all hydrogels. Agarose and PA at 6% exhibited the largest pattern enlargement with a pr/hd of 2.00 while the lowest distortion was observed in polyacrylamide-chitosan (PA-Chi), poly(ethylene glycol) diacrylate (PEGDA), and PEGDA-GelA with a pr/hd of 1.13. These differences in pattern resolution may result from different levels of affinity between the hydrogels and printing proteins. To test this hypothesis, hydrogels of different affinity to the printing molecules were tested. The results demonstrate that the higher the hydrogel-molecule affinity, the higher the pattern resolution. As expected, collagen-containing hydrogels exhibited patterns with higher resolution when using FN as the printing molecule[35] **(Figure S7)**. Furthermore, the stability of the patterns in time also depends on the specific hydrogel-molecule affinity **(Figure S8)**. Therefore, while the 3DEAL technique offers a high level of versatility with respect to the type of hydrogel and molecules used, the quality of the patterns will depend on the specific hydrogel-molecule combination.

These results demonstrate the capacity of the 3DEAL platform to move and localize molecules within multiple types of hydrogels to create deep patterns with micro-scale resolution and aspect ratios of up to 1:100 (diameter:depth), contributing to current efforts aiming to develop ever more complex scaffolds.[19-24,28,30,33,36] For example, creative methods developed by Ahadian et al. based on dielectrophoresis[37] and Dai using electrophoresis[30] have enabled patterning of aligned carbon nanotubes down to 50 μm in depth and nanoparticles down to 20 μm in depth, respectively. However, these techniques have been limited to using non-biological molecules and creating relatively shallow patterns within gels. Furthermore, Palleu et al. developed an ionoprinting technique that relies on cupper as an ion[31] for the patterning process, which could limit some biological applications.[38] Other groups have exploited the use of electric fields to directly pattern cells in 2D cultures using either DC[32] or in 3D using AC.[34] These approaches tend to require sophisticated facilities such as clean rooms for chip fabrication[32] and expose the cells to electrical field stresses.[34] Other methods based on UV irradiation,[20,22,23,28] covalent linkages,[39-40] and custom-made hydrogels[20,28,24,40,41] have been explored to create 3D patterns with more bioactive molecules. Pioneering light-triggered immobilization methods using for example stereolithography,[20] two-photon laser scanning photolithography,[42] or two photo-activated bioorthogonal reactions[28,41,42] have enabled patterning of peptides (RGDS)[28,40] and proteins (vitronectin)[44] within polyethylene-glycol hydrogels. However, these strategies depend on hydrogels with specific optical properties, have limited depth of printing, and require chemical modification of the hydrogel, the patterning molecule, or both. In contrast, the 3DEAL technique is simple,

capable of creating deep high aspect ratio patterns of multiple molecules including native proteins and within different types of readily available hydrogels, and relies on non-covalent interactions, which resembles the way ECM proteins interact.[45] The process may easily be adapted to print and pattern other molecules like polymers, which would further enhance the technique's potential to modulate the biochemical and physical complexity of the 3D environment.[45,46]

2.5. Patterning Complexity

The 3DEAL platform offers the possibility to generate molecular patterns of different sizes, geometry, and composition. For example, pattern geometry and resolution can be easily tuned by simply using masks with an appropriate permeability (as described above) and through-hole dimensions. Using a laser-patterned mask, bIgG patterns that were either 30 μm in diameter and 30 μm deep columns **(Figure 4a)** or 200 μm deep and 200 x 200 μm squared columns **(Figure 4b)** were fabricated in PA-GelA hydrogels. The later example demonstrates that, while a minor distortion is observed close to the mask, the squared geometry defined by the through-holes of the mask remains throughout the depth of the pattern **(Figure S9)**. In addition, the process can be extended to continuously print molecules up to centimetres in depth **(Figure 4c)**. These results demonstrate the capability of the 3DEAL technique to print molecules with low micrometre resolution, over large volumes, and with high geometrical control in all axes. Another advantage is the possibility to improve pattern complexity by simple modifications of the initial setup. By loading multiple molecules within the hydrogel prior to running the 3DEAL process we were able to pattern different molecules simultaneously and in specific locations **(Figure 4d-i)**. Slight

adjustments enable the fabrication of hydrogels with two or more molecules located either within the same pattern line **(Figure 4f)** or in patterns adjacent to each other **(Figure 4d and e)**. In this way, patterns with concentration gradients can be generated, including gradients of a single molecule or concentrations of two molecules that gradually transition from one molecule to another **(Figure 4g and h)**. By tuning the loading of two different molecules within the 3DEAL device, it is possible to fabricate hydrogels with regions of multiple concentrations of these molecules **(Figure 4h and i)**. In addition, by modifying the morphology of the hydrogel **(Figure 4j)** or placing additional electrodes at different positions within the hydrogel prior to the patterning process **(Figure 4k and l)**, it is possible to modify the electric field and consequently generate linear patterns with different geometries. The 3DEAL device also permits printing of molecules within hydrogels of different stiffness, including deformable soft gels. For example, printing 200 μm diameter columns of red fluorescently-labeled immunoglobulin G (rIgG) within PA-Colla 2%-0.1% hydrogels (5.47 Pa) enable protein patterns that can be manipulated to acquire different shapes **(Figure 4m)**. If two molecules of similar molecular weight (gIgG and rIgG) are loaded together **(Figure 4n)**, the resulting patterns will contain both molecules **(Figure 4o,p)**. Upon deformation of the soft gel, the straight patterns can be modified to take on desirable shapes (i.e. helical patterns) while maintaining the molecular anisotropy **(Figure 4p)**. It is important to mention, however, that given the versatility of the technique to pattern different types of hydrogels with multiple types of molecules of different molecular weight, variations in molecular concentration and patterning speed are likely to arise and would required specific tuning (**Figure S10**).

Other approaches such as bioprinting multilayered structures,[21] additive photopatterning,[22,23] 3D printing,[24] and sequential click reactions with photoaddition[28,29] have created complex patterns but tend to require sophisticated equipment and costly processes. The 3DEAL technique is simple, accessible, and enables the fabrication of precise and complex patterns from low μm to cm in size.

2.6. Cell Culture Scaffolds

Given the capability of the 3DEAL to pattern multiple types of hydrogels with multiple types of proteins, the technique may offer an attractive way to generate hydrogels with anisotropic chemical compositions that can be selectively recognized by cells. To evaluate this possibility, we patterned a polyacrylamide-collagen (PA-Colla) gel with circular columns of fFN + FN that were 150 μm in diameter and 800 μm in depth. We used the Colla and FN combination because of their mutual affinity and presence in the native ECM.[47-49] At day 4, cells were observed to be selectively adhering to the patterned regions **(Figure 5a and b)**, which demonstrates that protein functionality is maintained during the 3DEAL process. At day 14, immunofluorescence imaging confirmed that cells were spread and exhibited a well-formed actin cytoskeleton within the patterns down to about 100 μm in depth from the seeding point (top of the gel) **(Figure 5c-j)**. While the 3DEAL patterns provided FN paths for cells to migrate up to 800 μm, it is possible that cells did not penetrate beyond 100 μm due to the low porosity of the PA-Colla gel, which is known to have small pore sizes[50] and may affect cell and oxygen diffusion. Nonetheless, these results demonstrate the suitability of the 3DEAL for creating complex hydrogel

environments with functional macromolecules, within which cells could migrate, survive, and be anisotropically distributed.

3. Conclusion

We have developed an affordable, tuneable, and versatile fabrication process designed to print multiple types of functional molecules within different kinds of hydrogels with high precision and within large volumes. We have demonstrated the potential of the technique by generating complex molecular patterns made from native proteins within different widely used hydrogels. The functionality of the 3DEAL platform was assessed by selectively supporting NIH-3T3 cell growth on fibronectin patterns within a polyacrylamide-collagen hydrogel. The 3DEAL platform offers a simple, accessible, and practical method to create anisotropic environments with potential widespread applications in cell studies, *in vitro* models, drug screening, and tissue engineering.

4. Experimental Section

3DEAL Device: The 3DEAL device is simple and comprises two chambers for the buffer, two polyvinyl chloride (PVC) hose connectors, a capsule containing the hydrogel to be printed in, a printing solution and a mask that defines the printing geometry **(Figure 1)**. The PVC connectors were located at both ends of the capsule for connecting the capsule to the buffer chambers **(Figure 1d and e)**.

Masks: Regenerated cellulose (RC) dialysis membrane with a molecular weight cut off (MWCO) of 50 kDa and 3.5 kDa (Spectrum®Labs, USA) was cut into a sheet and used to make the masks. Two different methods were employed to make holes through the mask that would correspond to the final pattern geometry in the hydrogel. The first method is a manual procedure utilizing a sharp needle, resulting in the formation of circular through-holes of just over 150 μm in diameter. With this technique we fabricated twenty masks, two with a single circular through-hole in the mask center, five with circular through-holes making the letters of the 3DEAL, ten with 10 to 14 and four with 52 and 75 circular through-holes **(Supporting Section 4)**. The second procedure was used to improve reproducibility and precision of the through-holes on the mask. A femto-second pulsed laser source was used for selectively ablating the RC dialysis membrane with micrometric resolution and minimum thermal damage. With this technique we fabricated two masks with four 200 μm wide squares separated by 200 μm distances, and an array with twenty circles of 30 μm in diameter separated by 15 μm distances.

Capsules: Three slightly different capsules were designed and fabricated. The basic disposable capsule used for high-throughput patterning was made of two compartments including a flat polyethylene bottom compartment (FBC) (Ted Pella, Spain), which contains the hydrogel, and a 2 mL safe-lock tube (SLT) (Eppendorf, Spain) compartment, which contains the printing solution **(Figure 1a)**. Each capsule was filled with hydrogels in the pre-gel stage with 1 mL syringe (Becton, Dickinson and Company, Spain) **(Figure 1b)**. The capsule used for the visualization of the patterning process was made of two compartments including a glass tube (VWR International LTD, UK) that contains the

hydrogel and the PDMS tube that contains the printing solution **(Figure 1)**. An additional plastic strap clamps (VWR International LTD, UK) were used to secure the connection places from a potential leakage **(Figure 1)** prior to the filling of the glass tube with 2 mL of hydrogel in the pre-gel state, it was first plugged with a close-fit PDMS cork on one side. The capsule used for the patterning of soft hydrogels was custom made and comprised several compartments cut form PMMA, three metal rods facilitating the alignment of the PMMA compartments, and metal clamps that secure the capsule from a potential leakage **(Figure S1)**. The casting ring featured previously inserted holding membrane (50kDa MWCO; no holes) and was filled with 500 µL of hydrogel in pre-gel stage. Next, the metal rods were inserted into the previously drilled side-holes. Then a ring containing the mask was placed atop of the casting ring and additional 100 µL of the hydrogel in the pre-gel stage was added. Next, PMMA connecting compartments cut in a shape facilitating attachment of the capsule to the PVC hose were placed atop of the mask ring and the casting ring. Finally, three metal clamps were used to tighten the capsule.

Pattern Visualization: After the printing process, the resulting patterns within the hydrogels were visualized and characterized using a UV lamp and a Leica TCS-SP5 confocal microscope (Leica Microsystems, Germany), along with the ImageJ Software (NIH, USA) for reconstructing the 3D images.

Hydrogels: Six different polymers were used for the production of hydrogels including agarose novagel GQT (Pronadisa, Italy) at 3% w/v, polyacrylamide (PA) (BioRad,

Germany) at 2% v/v and 8% v/v, Poly(ethylene glycol) diacrylate (PEGDA) (Sigma-Aldrich, Spain) at 5% w/v; and polymer blends consisting of 6% v/v PA and 0.2% w/v gelatine type A (GelA) (Sigma-Aldrich, Spain), 6% v/v PA and 0.1% w/v chitosan (Chi) (Sigma-Aldrich, Spain) in 200 mM acetic acid, 6% v/v PA and 0.01% w/v collagen (Colla) from bovine calf (Sigma-Aldrich, Spain), and 5% w/v PEGDA with 0.1% w/v GelA. The PA, PEGDA, and the four blends were prepared by free-radical cross-linking polymerization with a monomer/cross-linker ratio of 20:1. Ammonium persulfate (APS) (Sigma-Aldrich, Spain) 10% was used as redox initiator and N,N,N′,N′-tetramethylethylenediamine (TEMED) (Sigma-Aldrich, Spain) as purchased was used as activator. All the hydrogels were prepared in a 10 mL final volume and then casted into the capsules. The polymerization process of each hydrogel lasted between 45 to 60 min at low oxygen atmosphere. The agarose hydrogel was prepared by mixing the agarose powder with the Tris-HCl buffer (Panreac, Spain) and subsequently heating in a microwave (Samsung, Germany) until a clear solution was obtained. The gelatine type A was prepared by adding the gelatine powder to a microwave-heated Tris-HCl buffer solution. The collagen was provided by the manufacturer dissolved in Acetic Acid at a final concentration of 3 $mgmL^{-1}$.

Buffer Solutions: The two buffer chambers were filled with 500 mL each of Tris/glycine buffer solution (2.5 mM/19.2 mM, pH 8.5). To prepare each hydrogel we used 375 mM Tris-HCl buffer at a pH of 8.8.

Printing Solution: The printing solution refers to the solution of the molecules to be printed. To be able to visualize the printed patterns, a blue fluorescently-labeled immunoglobulin G (bIgG) (KPL, USA), a red fluorescently-labeled immunoglobulin G (rIgG), a green fluorescently-labeled immunoglobulin G (gIgG) (BD, USA), and cow elastin full length protein (abcam, UK) as the molecules to be printed were used. For the cell attachment studies, fibronectin from bovine serum (FN) (Sigma-Aldrich, Germany) and fluorescent fibronectin from bovine serum (fFN) (Cytoskeleton-Inc., USA) were employed. The different proteins were mixed in 1% low melting Agarose in 375 mM Tris-HCl (pH 8.8) at 37 ˚C in order to hold in place the proteins to be printed within the capsule setup prior to the patterning process. The concentration of gIgG and bIgG was 12 μgmL^{-1} of the final seed solution for the PA and Agarose; for PEGDA 15 μgmL^{-1}; and 35 μgmL^{-1} for the PA-GelA, PA-Chi and PEGDA-GelA; finally for PA-Colla at 2% was 13 μgmL^{-1} of rIgG. For the cell attachment studies, 20 μgmL^{-1} of fFN were combined with 80 μgmL^{-1} of either PA-GelA or PA-Colla. For printing two molecules simultaneously, the molecules were loaded separately with 30 min interval to enable the agarose gel to set and thus avoid mixing of the molecules before the patterning process. To obtain patterns of two molecules within the same print line the molecules were loaded one on top of each other **(Figure 3)**, and to obtain the patterns of molecules adjacent to each other the molecules were loaded one next to each other **(Figure 3)**.

Patterning Process: For the patterning process, the 3DEAL device was connected to an electrophoresis source (Appelex, France) through two pieces of 8 cm long platinum wire as electrodes (Goodfellow, UK) submerged in the buffer solution. Each platinum wire was

situated at the opposite end of the buffer chambers. The wires were held in place by crocodile clips at the non-submerged ends, with each of these clips coupled to a cable connected to the electrophoresis source. Finally, the electrophoresis source was set to a constant voltage in the range of 150–200 V for an interval of 10 to 120 min. Additional modifications to the set up were made to obtain patterns of more complex geometries. To obtain bending patterns of the bIgG an additional 2 cm long platinum electrode in the form of 'U' letter was incorporated **(Figure 3)** where one side of the electrode was immersed in the middle of the hydrogel domain from the side (around 3 mm in depth), next 14 mm of the electrode were outside of the system, and the other side of the electrode was immersed back to the system through the PCV hose into the buffer solution on the side of the positive electrode. To obtain patterns of gIgG that form columns of the protein and then disperse into a surface vertical to the columns, an additional 2 cm platinum electrode in the form of a straight rod was incorporated **(Figure 3)** where around 15 mm were embedded in the centre of the hydrogel domain (around 10 mm from the mask) horizontally and the rest 5 mm were immersed in the buffer solution on the side of the positive electrode. Details of Numerical Simulations, Cell Culture and Cell Visualisation procedures are described in the *Section 9: Materials and methods* of the SI.

Supporting Information

Supporting Information is available from the Wiley Online Library or from the author.

Acknowledgements

Juan P. Aguilar and Michal Lipka contributed equally to this work. From the Experimental Toxicology and Ecotoxicology Platform at Parc Científic Barcelona, Spain, we thank Dr. Miquel Borras, Mr. Javier González, Mr. David Ramos, Mr. Joan Serret, Mr. Joaquin de Lapuente, and Ms. Alce Coloma. Also, we thank Dr. Miriam Royo from the Combinatorial Chemistry Platform, Dr. Eliandre de Olivera and Mr Ramón Díaz from the Proteomics Platform, both at the Parc Científic Barcelona; and Dr. Lídia Bardia and Dr. María Marsal from the Advanced Digital Microscopy Core Facility at the Institute of Research in Biomedicine. In addition we thank Mr. Carlos Edgardo Mendez for assistance with the illustrations. Finally, funding was provided by the ERC Starting Grant STROFUNSCAFF and the Government of Spain.

References

[1] S. Fisher, R. Tam, M. Shoichet, *Tissue Eng. Part A* **2014**, *20*, 895.

[2] M. Lutolf, J. Lauer-Fields, H. Schmoekel, A. Metters, F. Weber, G. Fields, J. Hubbell, *PNAS* **2003**, *100*, 5413.

[3] M. Zaman, L.Trapani, A. Sieminski, D. MacKellar, H. Gong, R. Kamm, A. Wells, D. Lauffenburger, P. Matsudaira, *PNAS* **2006**, *103*, 10889.

[4] S. Khetan, M. Guvendiren, W. Legant, D. Cohen, C. Chen, J. Burdick, *Nat. Mater.* **2013**, *12*, 458.

[5] S. Fraley, Y. Feng, R. Krishnamurthy, D. Kim, A. Celedon, G. Longmor, D. Wirtz, *Nat. Cell Biol.* **2010**, *12*, 598.

[6] F. Pampaloni, E. Reynaud, E. Stelzer, *Nat. Rev. Mol. Cell. Biol.* **2007**, *8*, 839.

[7] J. Zoldan, E. Karagiannis, C. Lee, D. Anderson, R. Langer, S. Levenberg, *Biomater.* **2011**, *32*, 9612.

[8] C. Fischbach, R. Chen, T. Matsumoto, T. Schmelzle, J. Brugge, P. Polverini, D. Mooney, *Nat. Methods* **2007**, *4*, 855.

[9] E. Gdor, S. Shemesh, S. Magdassi, D. Mandler, *ACS Appl. Mater. Interfaces* **2015**, *7*, 17985.

[10] S. Ahn, S. Jeon, E. Kwak, J. Kim, J. Jaworski, *Colloids Surf., B* **2014**, *122*, 851.

[11] H. Montón, M. Medina-Sánchez, J. Solera, A. Chałupniak, C. Nogués, A. Merkoçi, *Biosens. Bioelectron.* **2017**, *94*, 408.

[12] R. Kane, *Biomater.* **1999**, *20*, 2363.

[13] C. Wu, D. Reinhoudt, C. Otto, V. Subramaniam, A. Velders, *Small* **2011**, *7*, 982.

[14] E. Leclerc, K. Furukawa, F. Miyata, Y. Sakai, T. Ushida, T. Fujii, *Biomater.* **2004**, *25*, 4683.

[15] M. López-Bosque, E. Tejeda-Montes, M. Cazorla, J. Linacero, Y. Atienza, K. Smith, A. Lladó, J. Colombelli, E. Engel, A. Mata, *Nanotechnol.* **2013**, *24*, 255305.

[16] N. Choi, M. Cabodi, B. Held, J. Gleghorn, L. Bonassar, A. Stroock, *Nat. Mater.* **2007**, *6*, 908.

[17] Y. Li, K. Kilian, *Adv. Healthcare Mater.* **2015**, *4*, 2780.

[18] R. Perez-Castillejos, *Mater. Today* **2010**, *13*, 32.

[19] A. Wong, R. Perez-Castillejos, J. Christopher Love, G. Whitesides, *Biomater.* **2008**, *29*, 1853.

[20] R. Gauvin, Y. Chen, J. Lee, P. Soman, P. Zorlutuna, J. Nichol, H. Bae, S. Chen, A. Khademhosseini, *Biomater.* **2012**, *33*, 3824.

[21] J. Fernandez, A. Khademhosseini, *Adv. Mater* **2010**, *22*, 2538.

[22] V. Tsang, A. Chen, L. Cho, K. Jadin, R. Sah, S. DeLong, J. West, S. Bhatia, *FASEB J.* **2007**, *21*, 790.

[23] R. Tam, L. Smith, M. Shoichet, *Acc. Chem. Res* **2017**, *50*, 703.

[24] R. Truby, J. Lewis, *Nature* **2016**, *540*, 371.

[25] K. Inostroza-Brito, E. Collin, O. Siton-Mendelson, K. Smith, A. Monge-Marcet, D. Ferreira, R. Rodríguez, M. Alonso, J. Rodríguez-Cabello, R. Reis, F. Sagués, L. Botto, R. Bitton, H. Azevedo, A. Mata, *Nat. Chem.* **2015**, *7*, 897.

[26] S. Zhang, M. Greenfield, A. Mata, L. Palmer, R. Bitton, J. Mantei, C. Aparicio, M. De La Cruz, S. Stupp, *Nat. Mater* **2010**, *9*, 594.

[27] A. Mendes, K. Smith, E. Tejeda-Montes, E. Engel, R. Reis, H. Azevedo, A. Mata, A *Adv. Funct. Mater.* **2013**, *23*, 430.

[28] C. DeForest, B. Polizzotti, K. Anseth, *Nat. Mater.* **2009**, *8*, 659.

[29] V. Truong, M. Ablett, S. Richardson, J. Hoyland, A. Dove, *J. Am. Chem. Soc.* **2015**, *137*, 1618.

[30] X. Dai, S. Knupp, Q. Xu, Q. *Langmuir* **2012**, *28*, 2960.

[31] E. Palleau, D. Morales, M. D. Dickey, O. D. Velev, *Nat. Comm.* **2013**, *4*, 2257.

[32] D. J. Cohen, W. J. Nelson, M. M. Maharbiz, *Nat. Mater*. **2014**, *13*, 409.

[33] D. Albrecht, G. Underhill, A. Mendelson, S. Bhatia, *Lab Chip* **2007**, *7*, 702.

[34] S. Menad, L. Franqueville, N. Haddour, F. Buret, M. Frenea-Robin, *Acta Biomater.* **2015**, *17*, 107.

[35] J. R. Potts, I. D. Campbell, *Matrix Biol.* **1996**, *15*, 313.

[36] M. Sawkins, K. Shakesheff, L. Bonassar, G. Kirkham, *Recent Pat. Biomed. Eng.* **2013**, *6*, 3.

[37] S. Ahadian, J. Ramón-Azcón, M. Estili, X. Liang, S. Ostrovidov, H, Shiku, M. Ramalingam, K. Nakajima, Y. Sakka, H. Bae, T. Matsue, A. Khademhosseini, *Sci. Rep.* **2014**, *4*.

[38] B. Cao, Y. Zheng, T. Xi, C. Zhang, W. Song, K. Burugapalli, H. Yang, Y. Ma, *Biomed. Microdevices* **2012**, *14*, 709.

[39] S. Khetan, J. Burdick, *Biomat.* **2010**, *31*, 8228.

[40] Y. Luo, M. Shoichet, *Nat. Mater.* **2004**, *3*, 249.

[41] C. DeForest, E. Sims, K. Anseth, *Chem. Mater.* **2010**, *22*, 4783.

[42] A. Kloxin, A. Kasko, C. Salinas, K. Anseth, *Science* **2009**, *324*, 59.

[43] S. Lee, J. Moon, J. West, *Biomater.* **2008**, *29*, 2962.

[44] C. DeForest, D Tirrell, *Nat. Mater.* **2015**, *14*, 523.

[45] F. Rosso, A. Giordano, M. Barbarisi, A. Barbarisi, *J. Cell. Physiol.* **2004**, 199, 174.

[46] J. Mouw, G. Ou, V. Weaver, *Nat. Rev. Mol. Cell Biol.* **2014**, *15*, 771.

[47] M. Vuento, E. Salonen, K. Osterlund, U. Stenman, *Biochem. J.* **1982**, *201*, 1.

[48] M. Erat, B. Sladek, I. Campbell, I Vakonakis, *J. Biol. Chem.* **2013**, *288*, 17441.

[49] S. Chandrasekhar, J. Sorrentino, A. Millis, *PNAS* **1983**, *80*, 4747.

[50] L. Haggerty, J. Sugarman, R. Prudhomme, *Polymer* **1988**, *29*, 1058.

Received: ((will be filled in by the editorial staff))

Revised: ((will be filled in by the editorial staff))

Published online: ((will be filled in by the editorial staff))

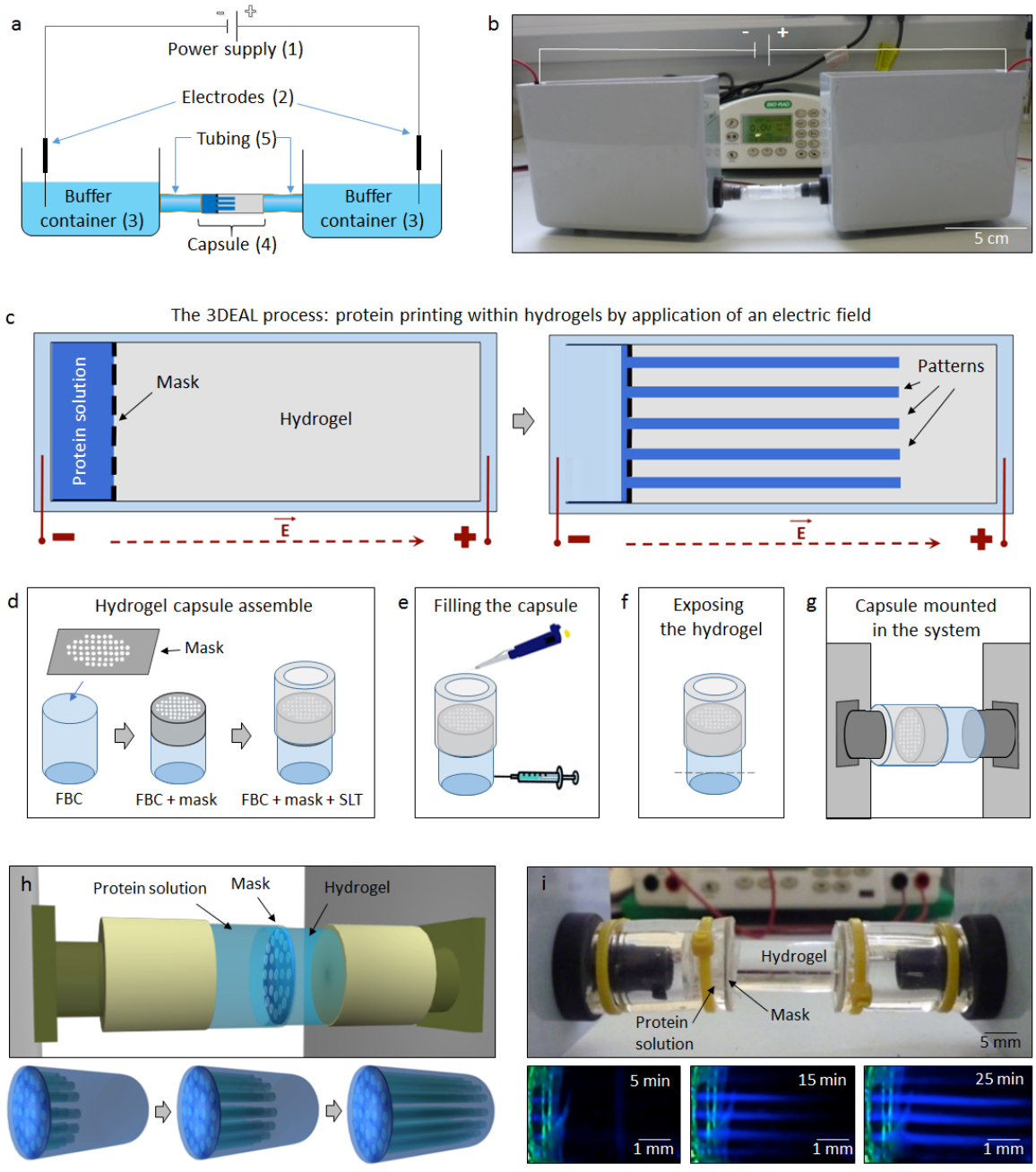

Figure 1. 3D Electrophoresis-Assisted Lithography (3DEAL) components and patterning process. (a), Schematic and **(b),** photograph of the assembled 3DEAL platform highlighting the 5 key components. **(c),** Schematic of the capsule before and after the patterning process comprising the protein solution, mask, electrodes, and hydrogel. The application of the electric field (EF) drags the printing molecules through the hydrogel generating patterns of specific size and shape defined

by the through-holes of the mask. Schematics of **(d-g),** the steps required for the assembly of the capsule made of a mask, flat bottom capsule (FBC), and a safe lock tube (SLT) **(d)**, filling with the protein solution and the hydrogel **(e)**, exposing of the hydrogel **(f)**, and attachment to the containers of the buffer solution **(g)**. **(h),** Schematic of a closer view of the assembled hydrogel capsule (top) and graphical representation of the hydrogel during printing (bottom). **(i),** Photograph of the glass hydrogel capsule (top) and time-lapse fluorescent images of the hydrogel during the patterning process (below).

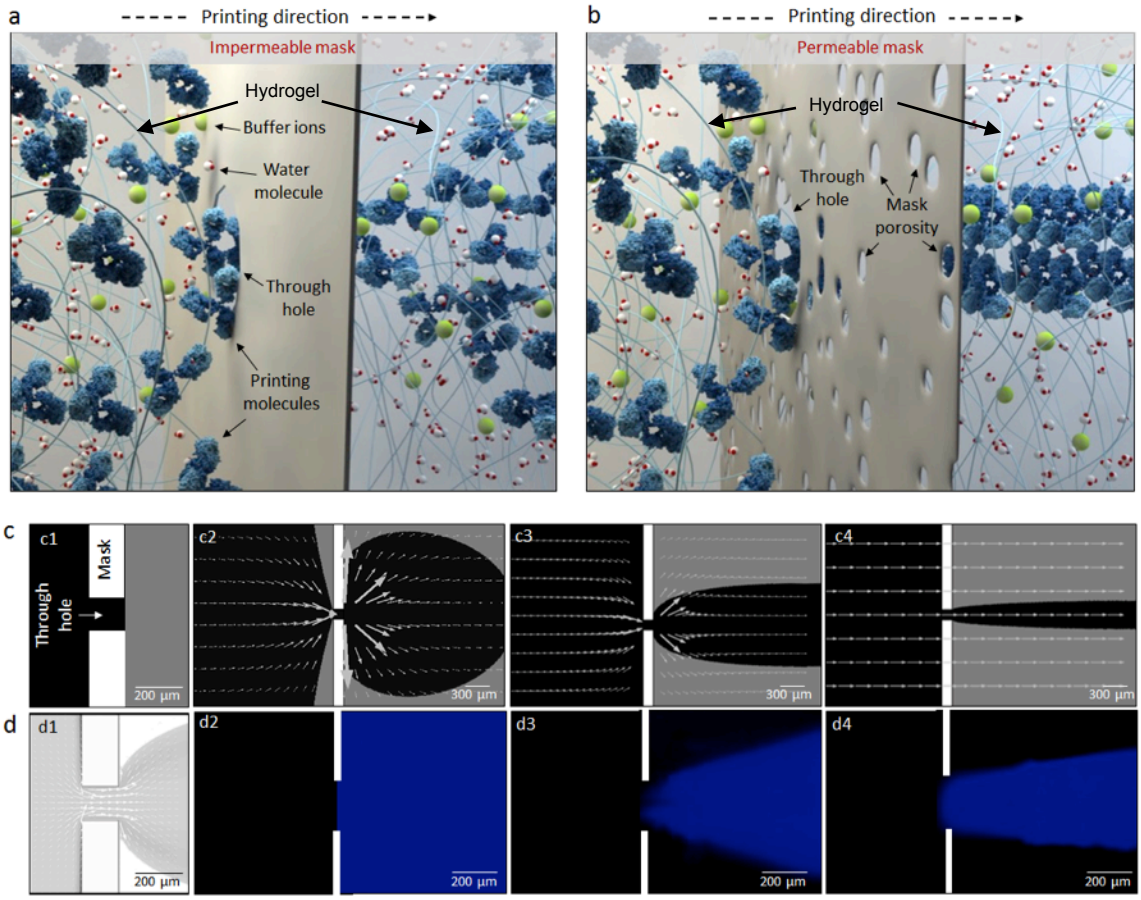

Figure 2. Mask permeability and directional control of the electric field during the 3DEAL. **(a), (b),** Graphical representations of the 3DEAL at the interface of the printing solution, mask with one through-hole, and hydrogel illustrating the fundamental elements required for the process including printing molecules, water molecules, and buffer ions, using an impermeable non-porous mask **(a)** and a permeable one **(b)**. Appropriate permeability of the mask is essential to control the direction of the electric field and printing molecules. Numerical simulations **(c)** and experimental results using bIgG as printing molecule and a PA-GelA hydrogel **(d)** from an experiment using a mask with one through-hole and either no **(c2, d2)**, low **(c3, d3)**, and high **(c4, d4)** permeability. The numerical simulations demonstrate the velocity field distribution (the directionality and size of the white arrows indicate the electric field direction and speed increment) across the three types of masks and the resulting pattern as a result of the level of permeability **(c2-c4)**. Fluorescent images

of bIgG patterns produced in PA-GelA hydrogels using either a PDMS (non-permeable) mask **(d2)**, a 3.5 kDa MWCO (low permeability) mask **(d3)**, or a 50kDa MWCO (high permeability) mask **(d4)**. The results demonstrate the importance of an optimum mask permeability that enables passing across the mask of water molecules and ions of the buffer and blocking of the printing molecule across at the through-hole of the mask.

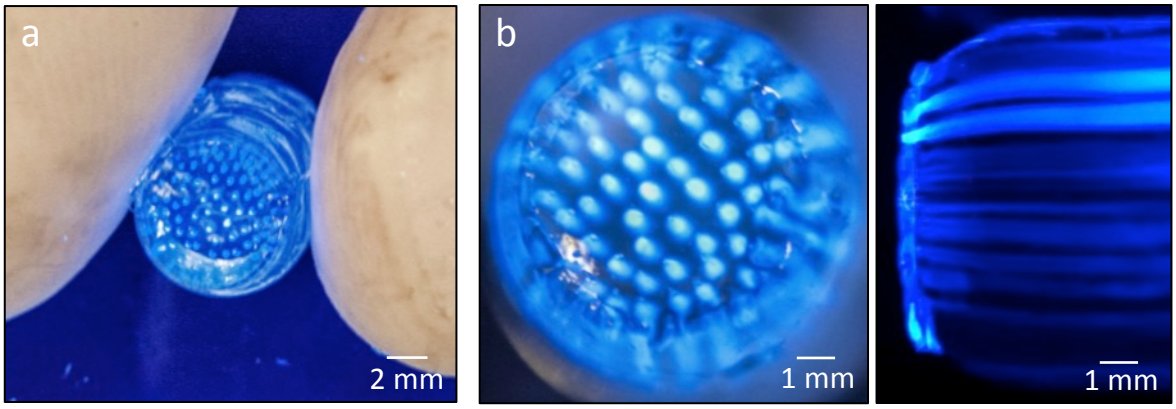

Material	Affinity	Concentration	Time	Voltage	Protein	pr/hd
When pattern Molecule was: bIgG, gIgG or rIgG						
PA	NO	2%	20min	150 V	12 µg	6.66
PA-GelA	Medium	2%-0.1%	45min	150 V	13 µg	3.33
Agarose	NO	2%	10min	150 V	12 µg	2.00
PA	NO	8%	15 min	150V	12 µg	1.67
PEGDA	Low	5%	20 min	150 V	15 µg	1.27
PA-GelA	Medium	6%-0.1%	35 min	150 V	35 µg	1.20
PA-Chi	Medium	6%-0.1%	35 min	150 V	35 µg	1.13
PA-Colla	Medium	6%-0.1%	35 min	150 V	35 µg	1.13
PEGDA-GelA	Medium	5%-0.1%	35 min	150 V	35 µg	1.13
When Pattern Molecule was: FN or fFN						
PA-Colla	High	6%-0.01%	45 min	150 V	100 µg	1.00

Figure 3. **Performance and versatility of the 3DEAL platform. (a),** Patterned PA-GelA hydrogel being held, exhibiting bIgG patterns of 150 µm in diameter and 5 mm in depth **(b)**. The bottom panel summarizes the processing conditions and printing performance using 10 different hydrogels by quantifying the difference between the diameter of the mask through-hole (hd) and the cross-sectional area of the pattern within the hydrogel (pr).

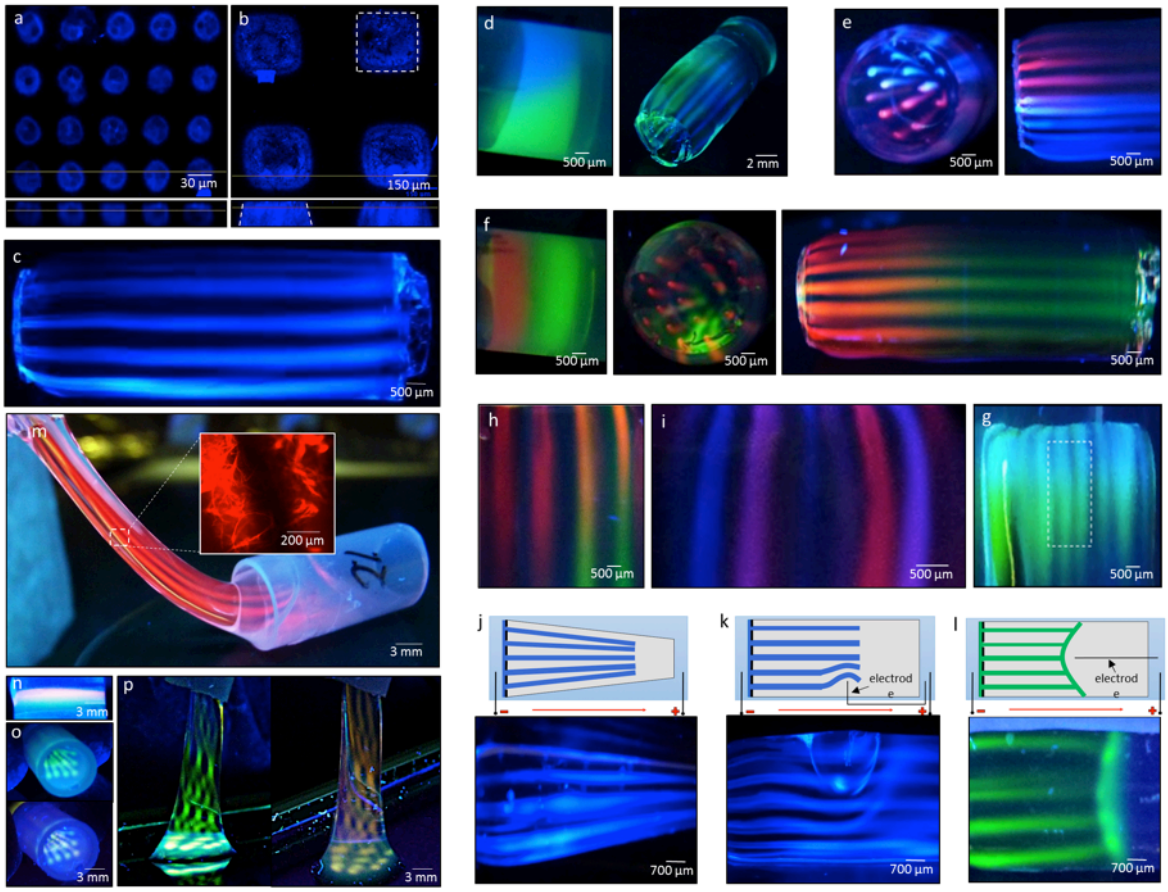

Figure 4. **3DEAL capabilities and printing complexity. (a),** Fluorescent images of an array of circular 30 µm diameter and its cross-section view of the fourth row; and 200 µm x 200 µm squared patterns and its cross-section view of the second row **(b)** patterns of bIgG printed within PA-GelA. The images were taken after 10 days of incubation in 37 ˚C in PBS 1X to demonstrate the stability of the patterns. The dotted lines indicate a slight lateral dispersion immediately after the mask **(b)**. A PA-GelA hydrogel printed with high aspect-ratio bIgG patterns (150 µm in diameter/2 cm in depth) **(c)**. Hydrogels with multiple molecules including either gIgG and bIgG **(d)** or rIgG and gIgG **(e)** being printed adjacent to each other or within the same pattern line using rIgG and elastin **(f)**. **(g-i),** PA-GelA hydrogels with complex multi-molecular patterns including concentration gradients being generated from bIgG patterns transitioning into gIgG patterns **(g)**; printed areas with multiple molecules including rIgG patterns (red), elastin patterns (green), and areas with both molecules

(orange) **(h)**; and patterns with different concentrations of bIgG and rIgG depicted by patterns of different colours **(i)**. Schematics (top) and side views (bottom) of the patterns obtained within PA-GelA hydrogels after slight modifications of the capsule including a hydrogel with a conical geometry **(j)**, additional electrode in the centre of the hydrogel **(k)**, and additional electrode on the side of the hydrogel **(l)**. Distorted soft PA-Colla 2%-0.1% hydrogel with printed cylindrical patterns of rIgG **(m)**. **(n-p)**, PA-Colla with complex multi-molecular patterns from gIgG and rIgG. The hydrogel could be moulded into different shapes, such as helical patterns, maintaining the pattern complexity and definition **(p)**.

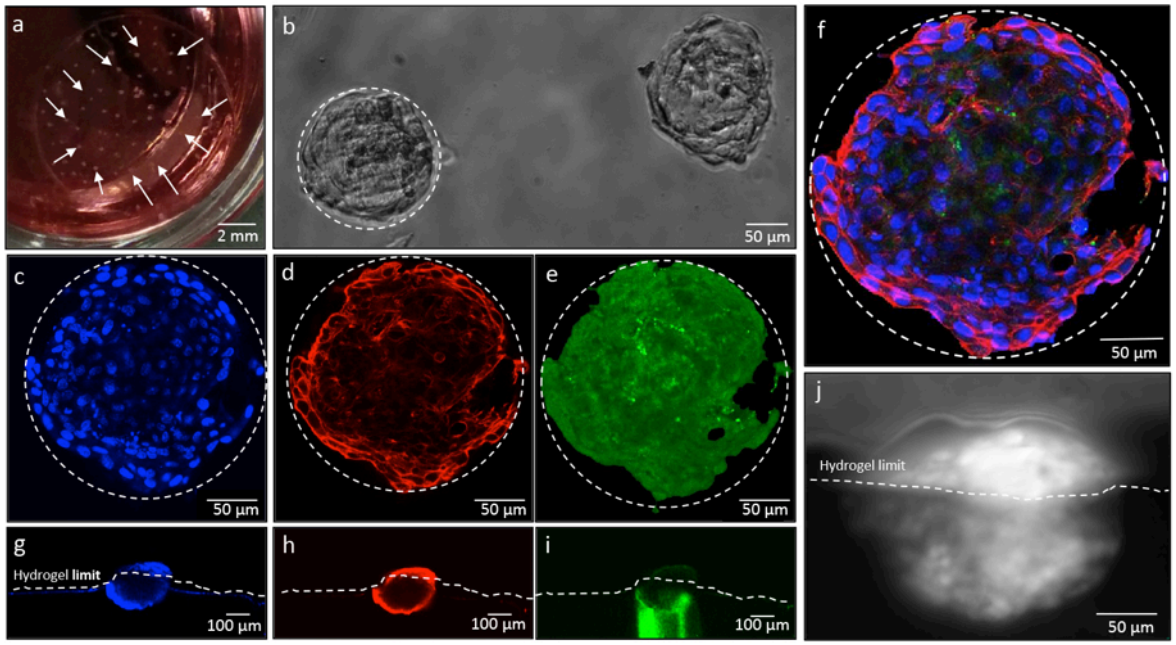

Figure 5. Functionality of the 3DEAL platform. (a), NIH-3T3 cell recognition of fFN+FN patterns within PA-Colla hydrogel after days in culture where the arrows indicate cell clusters located on the patterned areas. **(b),** Magnification of two cell clusters under bright field. Immunofluorescent microscopy images of a cell cluster showing the cell nuclei (blue) **(c)** and actin cytoskeletons (red) **(d)** directly on the 200 µm-diameter fFN+FN pattern (green) **(e)**. **(f),** Overlapping all three images, demonstrating pattern recognition by the cells. **(g-j),** The cluster's cross-sectional views depicting the cells growing down to about 100 mm in depth.

The 3D electrophoresis-assisted lithography (3DEAL) is an affordable, tuneable, and versatile fabrication process designed to print multiple types of functional molecules within different kinds of hydrogels with high precision and within large volumes. The 3DEAL platform enables chemically anisotropic environments with microscale resolution and tuneable geometry.

Keyword: 3D patterning, molecular printing, electrophoresis, lithography, anisotropic hydrogels

J. P. Aguilar, M. Lipka, G. A. Primo, E. E. Licon-Bernal, J. M. Fernández-Pradas, A. Yaroshchuk, F. Albericio, A. Mata*

3D Electrophoresis-Assisted Lithography (3DEAL): 3D molecular printing to create functional patterns and anisotropic hydrogels

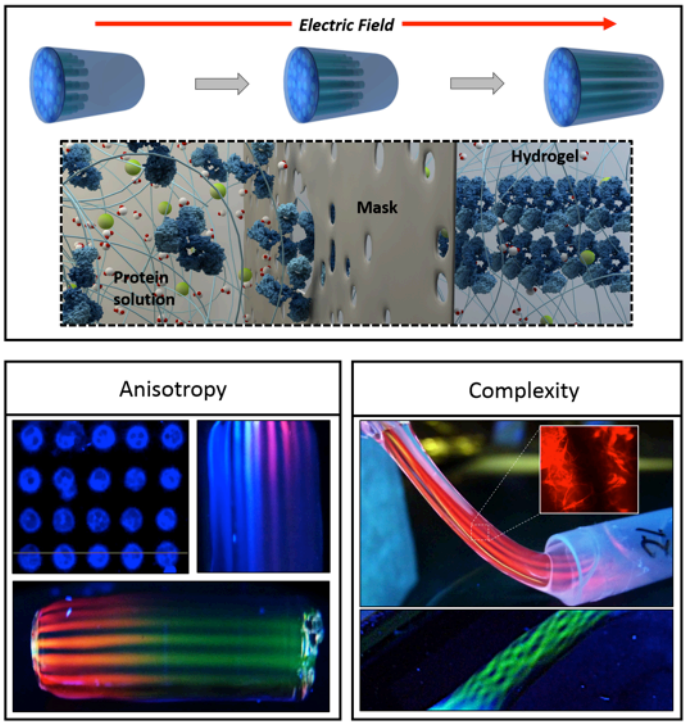

Supporting Information

3D Electrophoresis-Assisted Lithography (3DEAL): 3D molecular printing to create functional patterns and anisotropic hydrogels

*Juan P. Aguilar, Michal Lipka, Gastón A. Primo, Edxon E. Licon-Bernal, Juan M. Fernández-Pradas, Andriy Yaroshchuk, Fernando Albericio, Alvaro Mata**

Supporting Information Contents:

Supporting Section 1. The configurations of the capsules.

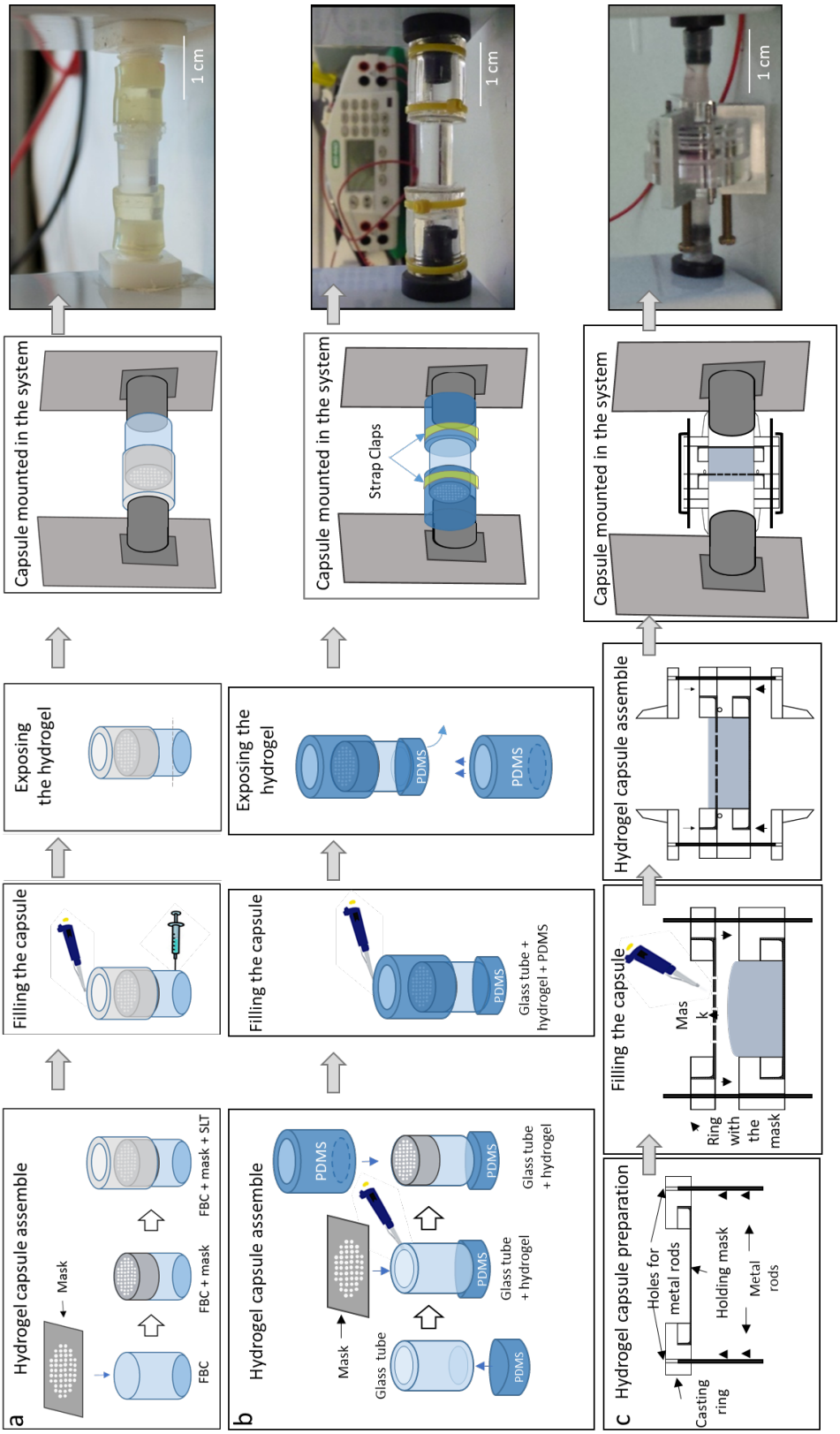

Figure S1. Schematic of the different configurations of the capsules used in the 3DEAL technique comprising the protein solution, mask, and hydrogel. **(a),** Basic configuration made by combining a mask, flat bottom capsule (FBC), and safe lock tube (SLT). **(b),** Glass configuration made by combining a glass tube and two pieces of Polydimethylsiloxane (PDMS) with plastic strap clamps for holding the mask and preventing leaking during the polymerization process. **(c),** PMMA configuration of the PMMA chambers for the hydrogel and the printing solution. Each row of the figure summarizes the filling process of the capsule with the hydrogel and the corresponding printing solution; followed by exposure of the hydrogel at the bottom and the assembly of the capsule. Finally, the real assembled device of the 3DEAL setup is presented, with a close-up of each hydrogel capsule assembled to the buffer chambers.

Supporting Section 2. The versatility of the 3DEAL platform.

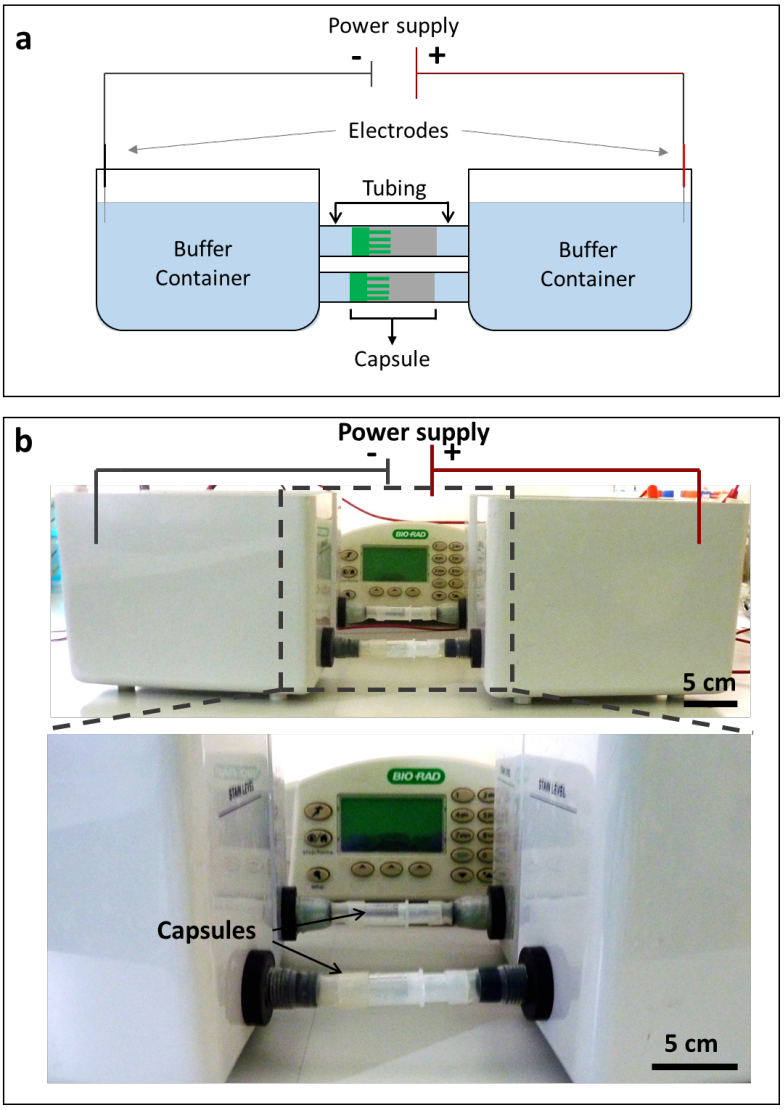

Figure S2. Tuneability of the 3DEAL platform. The platform facilitates the modification of the arrangement and disposition of the components based on the user requirements. **(a),** Schematic and **(b),** photograph of a parallel arrangement of capsules within the platform. Two capsules are connected to the same power supply and buffer containers.

Supporting Section 3. Governing equations.

To resolve the Numerical Simulations (NS), continuity equations for the flow velocity and the current density at steady state are taken into account as:

$$\nabla \cdot \mathbf{u} = 0 \quad ; \quad \nabla \cdot \mathbf{I} = 0 \qquad \text{(S1)}$$

Here u, denotes the velocity vector (m/s) and I represents the current density vector (A/m^2). The velocity includes two driving force, a pressure term and an electroosmotic term:

$$\boldsymbol{u} = \mathrm{P}_H \nabla p + \mathrm{P}_{EO} \nabla \mathrm{V} \quad ; \quad P_H = \frac{\varepsilon_p a^2}{8\mu\tau} \quad ; \quad P_{EO} \frac{\varepsilon_p \varepsilon_w \zeta}{\mu\tau} \qquad \text{(S2)}$$

Where P_H and P_{EO} are respectively, hydrulic and electroosmotic permeability and they are diferent in the gel and in the membrane. In equation 2, ε_p denotes the porosity, a is the average radius of the pores (m), μ gives the fluid's dynamic viscosity (Pa·s), τ represents the tortuosity of the porous structure, ε_w is the fluid's permittivity (F/m), p gives the pressure (Pa), ζ is the zeta potential (V), and V is the potential (V). The current density is given by:

$$\mathbf{I} = -\mathrm{k}\,\nabla \mathrm{V} \qquad \text{(S3)}$$

where κ denotes the conductivity (S/m).

the boundary conditions are given for this case at the inlet and the outlet, the pressure is fixed and at the solid walls the normal velocity component vanishes:

$$p(r,0) = p_1 \quad ; \quad p(r,L) = p_2 \quad ; \mathbf{n} \cdot \mathbf{u} = 0 \text{ at the walls} \qquad \text{(S4)}$$

In turn, boundary conditions for the current-density balance are insulating for all boundaries except at the inlet and the oulet, where the potential is fixed

$$\mathbf{n} \cdot \mathbf{I} = 0 \text{ at the walls} \; ; \; V(r,0) = V_1 \quad ; \quad V(r,L) = 0 \qquad \text{(S5)}$$

In the second model stage, the steady-state velocity and potential fields are used in a transient simulation of the concentration of a charged tracer species injected into the system, assuming that the tracer species does not influence the conductivity or the set potential in the porous structure. The mass-transport equation for the tracer read

$$\frac{\partial c}{\partial t} + \nabla \cdot \mathbf{N} = 0 \qquad \text{(S6)}$$

where N is the flux vector given by the Nernst-Planck equation:

$$\mathbf{N} = -D\nabla c - zu_m Fc\nabla V + c\boldsymbol{u} \qquad \text{(S7)}$$

In this equation, D denotes the tracer's diffusivity (m^2/s), c gives its concentration (mol/m^3), z represents the tracer's charge number, and F is Faraday's constant (C/mol). The mobility, u_m ($mol \cdot m^2/(J \cdot s)$), is given by the Nernst-Einstein equation:

$$u_m = \frac{D}{RT} \qquad \text{(S8)}$$

where R=8.314J/(mol·K) is the gas constant and T(K) is the temperature. The boundary conditions for the mass-transport equation, are insulating for all the walls including the membrane. At the inlet a given constant concentration and at the outlet an outflow condition. The Flux condition is used to set the diffusive and convective contributions to the flux through the boundaries to zero:

$\mathbf{n} \cdot \mathrm{N} = 0$ at the walls and membrane ; $\mathbf{n} \cdot (-\mathrm{D}\nabla \mathrm{c} + \mathrm{c}\mathbf{u}) = 0$ at the oulet ; $c(r, 0) = c_1$

(S9)

in order to simplify the numerical simulation, an initial concentration distribution uniform in the radial coordinate and bell-shaped in the longitudinal direction has to be set:

$$c(r, Z, t = 0) = c_1 * exp(-8\frac{Z}{L}) \qquad \text{(S10)}$$

Supporting Section 4. Mask and pask permeability.

Mask

The mask used for the 3DEAL technique is made from Standard Grade Regenerated Cellulose (RC) dialysis membranes (Spectra/Por® 7 – Spectrum®Labs, USA). These membranes are manufactured from natural cellulose reconstituted from cotton linters. These membranes do not exhibit charge, prevent solute absorption, and are chemically treated to minimize heavy metal and sulfur content. The specifications for use from the manufacturer include a pH range between 2-12, temperatures below 60 °C, and can be used with organic solvents. Some recommended solvents for using this membrane are hydrochloric acid (diluted), triethylamine, and water among others.[1]

Molecular Weight Cut-Off selection: As general practice, the supplier (Spectrum®Lab) suggests a selection of membrane Molecular Weight Cut-Off (MWCO) that is 50-80% of the molecular weight of the macromolecule to be retained **(Figure S3)**.[1]

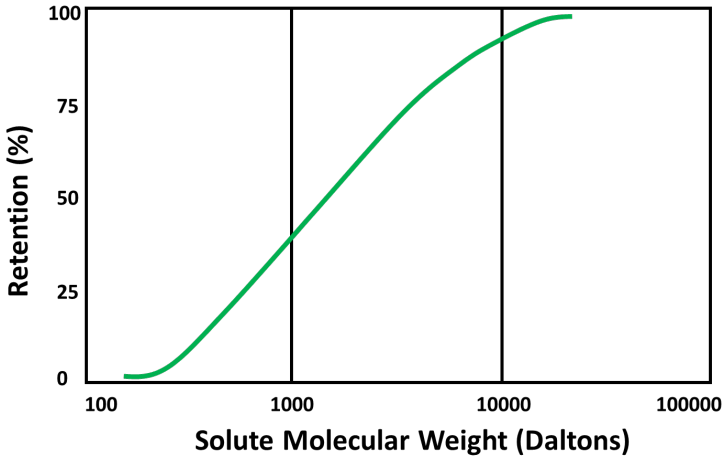

Figure S3. Retention plotted against solute molecular weight. For choosing the MWCO of a membrane to be used to fabricate a 3DEAL mask, a solute should be retained near to

100%. Based on the manufacturers specifications, to retain a 10 kDa solute and enable high definition patterning using the 3DEAL technique, a membrane of ~1.2 kDa should be used. (Adapted from Fundamentals of Membrane Dialysis - http://spectrumlabs.com/dialysis/Fund.html).

As speicified by the manufacturer, while there is no direct correlation between pore size and molecular weight, **(Figure S4)** represents a good approximation for an estimated conversion between these two variables.

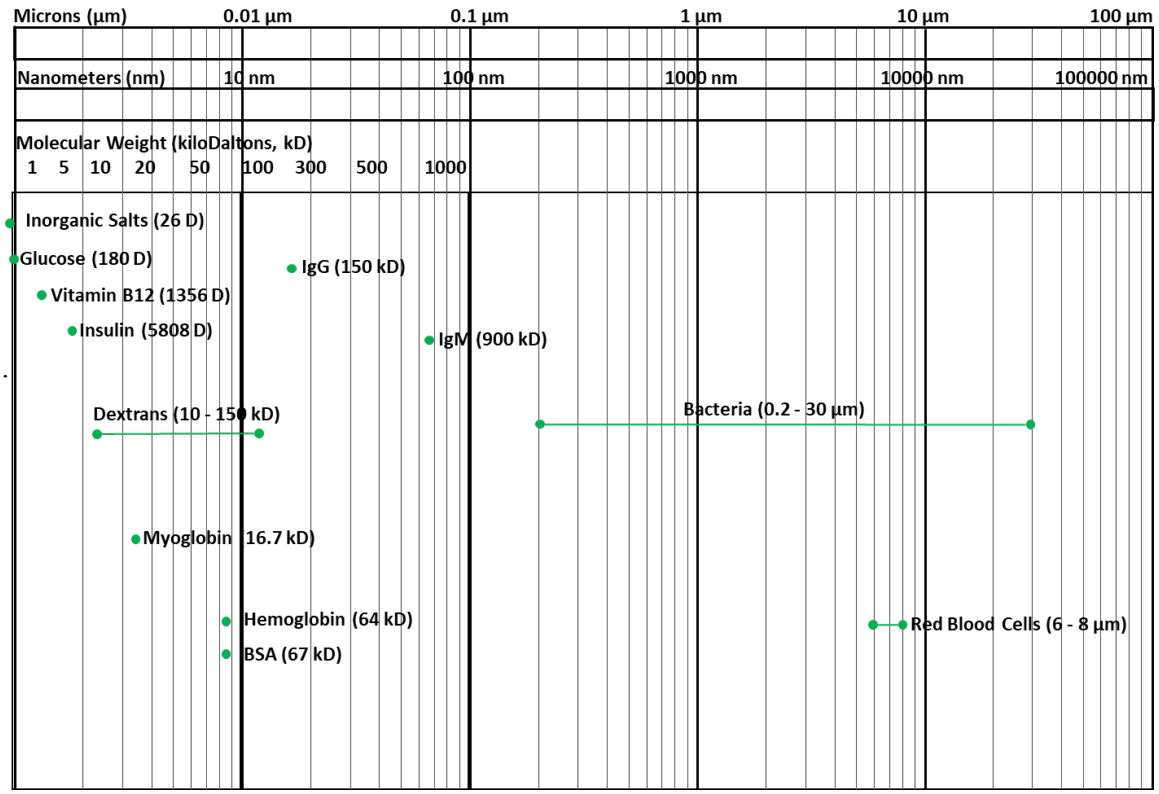

Figure S4. Size chart. Correlation between pore size (nm/µm) and molecular weight (kDa) of different entities. (Adapted from Fundamentals of Membrane Dialysis - http://spectrumlabs.com/dialysis/Fund.html).

Mask Micrography

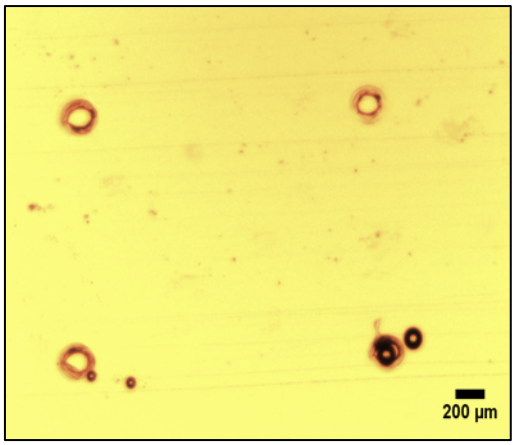

Figure S5. Mask. Micrograph of a patterned mask (dialysis membrane 50 kDa MWCO) with through holes of ~150 µm diameter. The black round-like shapes are water bubbles trapped between the mask and the cover slip.

Mask permeability

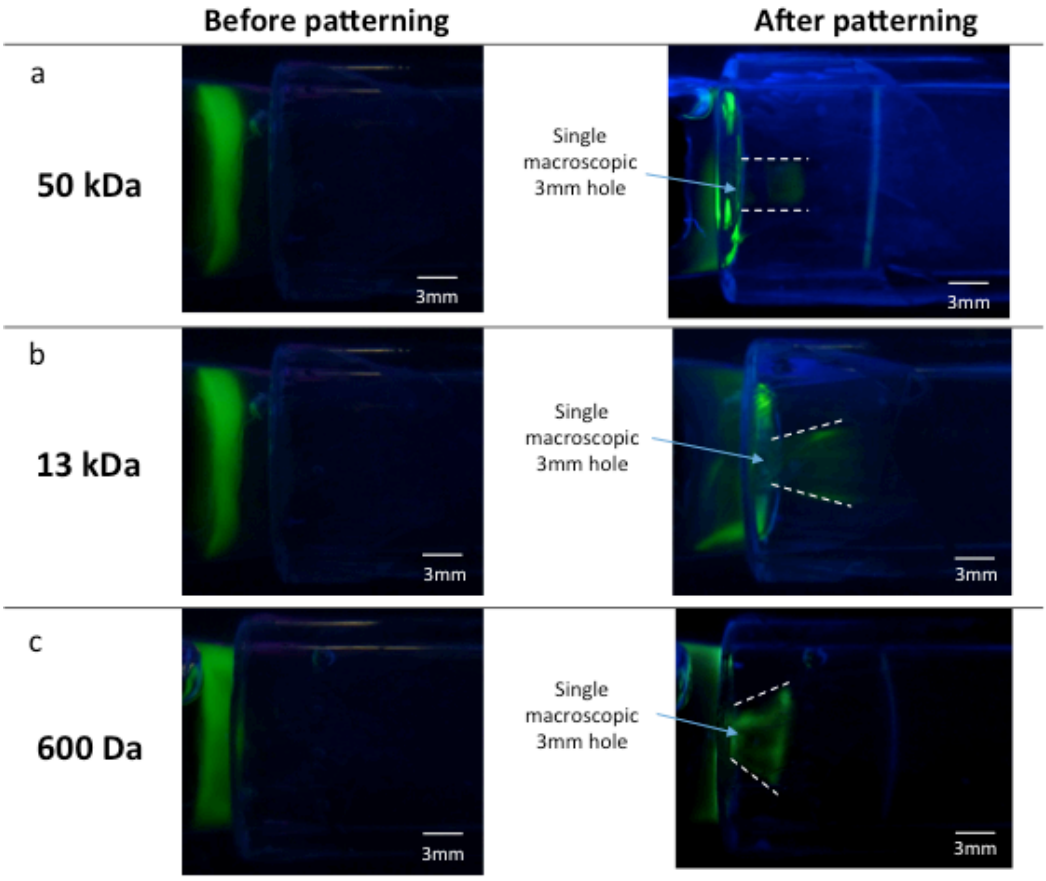

Figure S6. Fluorescent images of gIgG patterned PA-GelA hydrogel using masks made from different regenerated cellulose (RC) and esther cellulose (EC) membranes with different molecular weight cutoff (MWCO) with a through-hole of 3 mm; in the glass configuration. Each mask has different level of permeability. **(a),** 50 kDa MWCO RC (high permeability) **(b),** 13 kDa MWCO RC (middle permeability) mask and **(c),** 600 Da EC (very low permeability). The images from the left side were taken in a moment before the printing molecule reached the mask; otherwise the right side images were obtained 10 minutes after the printing molecule cross the mask. The results support the importance of an optimum mask permeability that enables passing across the mask of water molecules

and ions of the buffer and blocking of the printing molecule across at the through-hole of the mask; to obtain a good control of the form given by the mask through-hole.

Supporting Section 5: Protein pattern resolution.

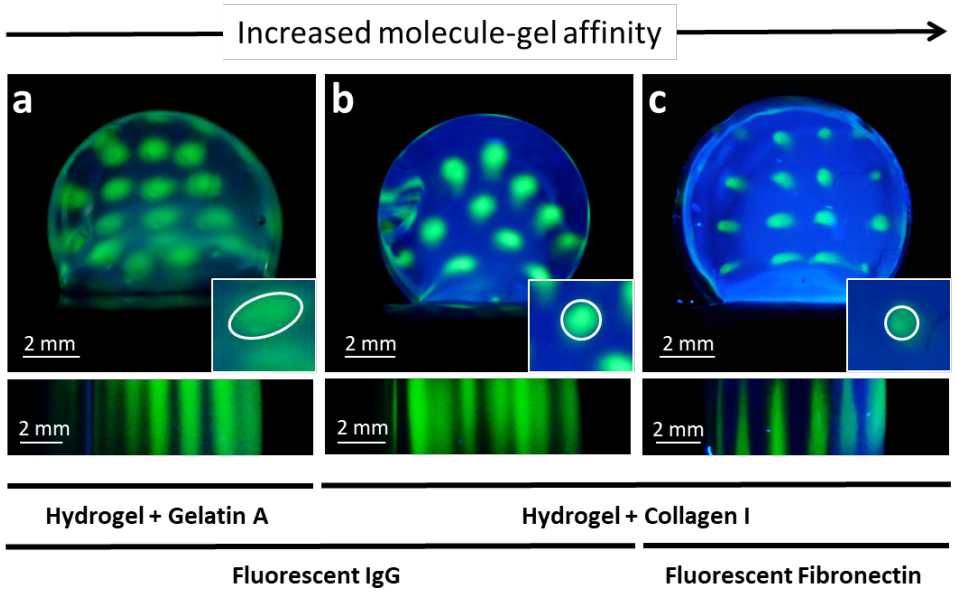

Figure S7. Pattern affinity and resolution. The patterns are more defined (from left to right) as the level of affinity between the hydrogel and the printing molecule increase. **(a),** PA-Gel A 3%-0.01% printed with gIgG, **(b),** PA-Colla 3%-0.01% printed with gIgG, and **(c),** PA-Colla 3%-0.01% printed with fFN+FN. Top images depict front views while bottom ones side views. Inset: zoom of a pattern spot. The white ring highlights a single pattern.

Supporting Section 6. Pattern stability.

The stability and definition of the patterns in time depends on the specific affinity between printed proteins (or molecule) and hydrogels. Collagen hydrogels, thanks to their free amine groups and secondary structure, offers a good anchor point for proteins. As it is shown in **(Figure S8a)**, collagen hydrogels maintain printed IgG patterns stable up to 7 days. On the other hand, agarose, a polysaccharide without specific binding sites for proteins, does not offer a good binding affinity for the printed proteins. **(Figure S8e)** depicts the lack of affinity of IgG for agarose, observing the complete diffusion of the patterns in only 4 hours of soaking in PBS 1X. The mixture between agarose and collagen **(Figure S8d)** offers a good compromise situation in pattern stability both in time and in maintaining their definition.

In addition, there is a clear dependence on patterns stability upon the storing conditions. Storing at low temperatures **(Figure S8a)**, maintained the patterns stable up to 7 days but some diffusion of the non-specifically bound proteins was observed. Whereas, storing at 37 °C avoids the initial protein diffusion but reduces the overall stability **(Figure S8c)**. Chemically immobilization of the patterned proteins within the hydrogel with paraformaldehyde 4% offers, on one hand, the possibility to minimize the diffusion of the non-specifically bound proteins; and on the other hand, allows a good stability over time **(Figure S8d)**.

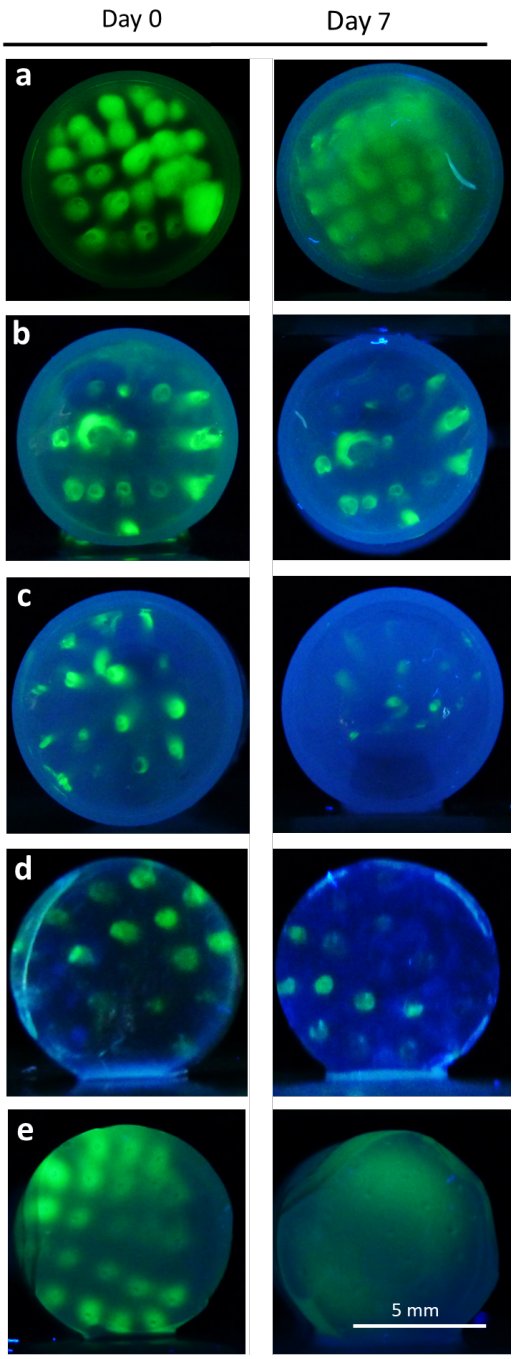

Figure S8. Stability of patterns after 7 days for different hydrogels and conditions. (a), Collagen 1 mg/mL printed with gIgG at 200V for 1.5 h, soaked in PBS 1X and stored at 5 °C. **(b),** Collagen 1 mg/mL printed with gIgG at 200V for 1.5 h, fixed with paraformaldehyde 4% for 30 min and stored at 5 °C in PBS 1X. **(c),** Collagen 1 mg/mL

printed with gIgG at 200V for 1.5 h, soaked in PBS 1X and stored at 37 °C. **(d),** Agarose 1% - Collagen 0.5 mg/mL printed with gIgG at 100V for 45 min, soaked in PBS 1X and stored at 5 °C. **(e),** Agarose 1% printed with gIgG at 100V for 45 min, soaked in PBS 1X and stored at 5 °C. The **Day 0** column represents the hydrogels immediately after the patterning process while the **Day 7** column represents the same hydrogel 7 days after patterning. An exception should be done with **(e)**, for which the **Day 7** column represents only 4 hours of storing.

Supporting Section 7. Conservation of the squared geometry pattern.

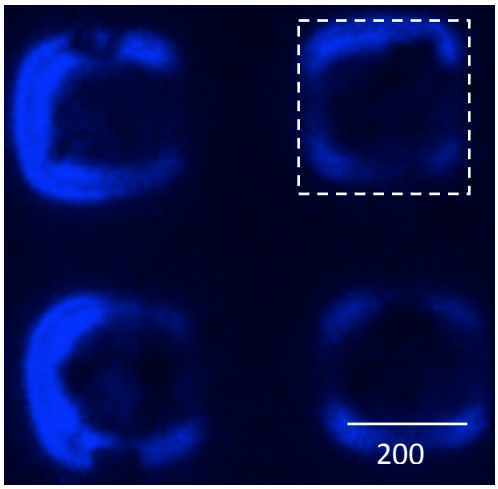

Figure S9. Fluorescent images from **(Figure 4b)** at 200 µm depth from the bottom. It is possible to validate how the squared shape of the pattern is preserved.

Supporting Section 8. Protein characterization.

We used image analysis (Fiji-ImageJ, NIH, USA) to measure the intensity of the protein patterns and provide insight into their relative concentrations after the patterning process. The patterning process produces a gradient with decreasing relative concentration with higher concentration closer to the mask and lower as the pattern moves away from the **(Figures S10a-c)**. The protein solution acts as a "protein reservoir" enabling a constant supply of protein as the process occurs. Due to this reservoir, it is likely that as the pattern develops, areas closer to the mask are more exposed to proteins over time **(Figure S10a-c)**. When two proteins of different molecular weight (MW) are seeded together and printed at the same time, they will migrate at different rates with the molecule with lower MW migrating faster. This effect can be observed when using a mixture of elastin (green) exhibiting a lower molecular weight compared to an IgG protein (red), as observed when performing an RGD deconvolution of the patterns **(Figures S10d-f)**. However, the general trend mentioned above of a decreasing relative protein concentration is maintained.

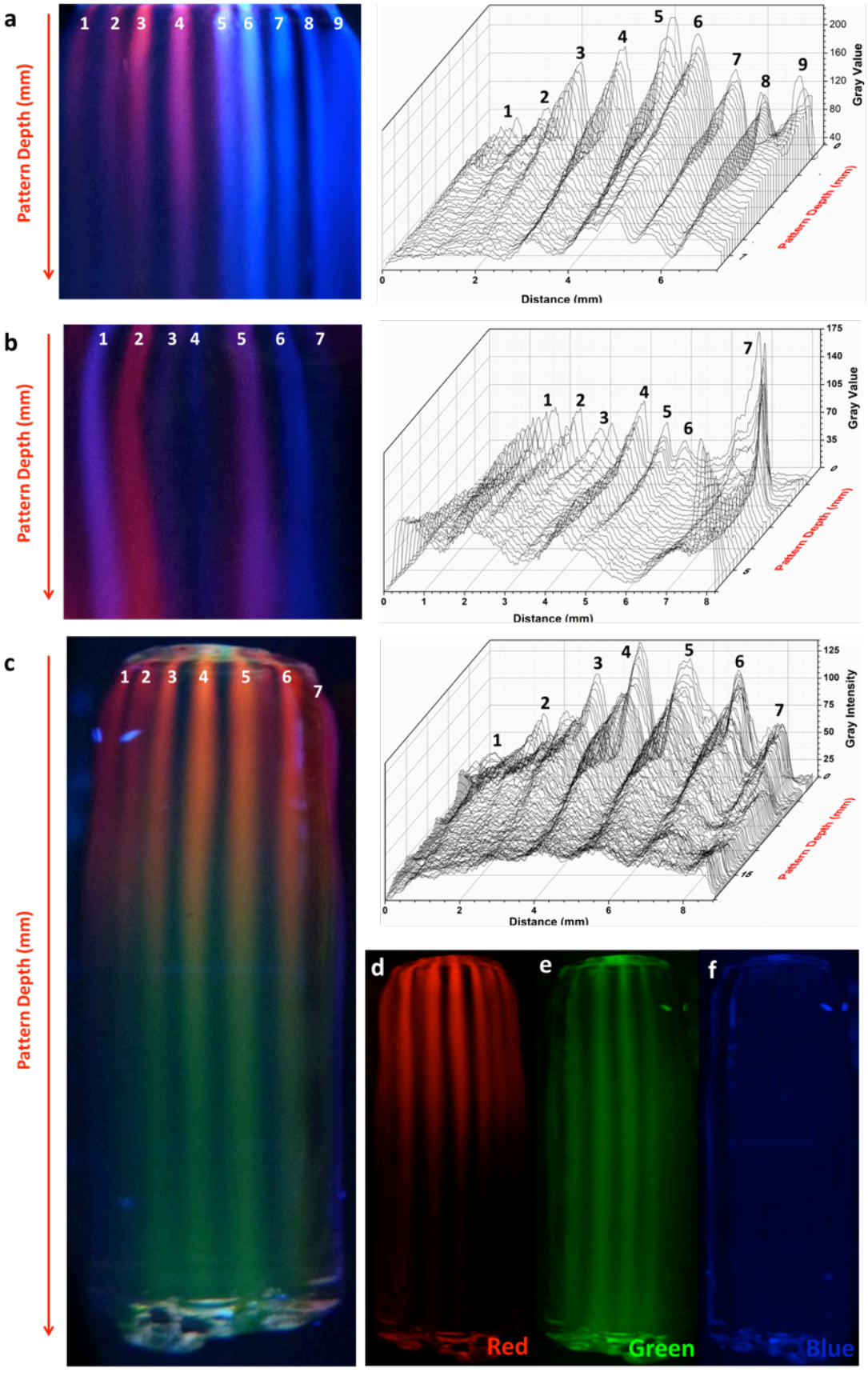
a
1 2 3 4 5 6 7 8 9
Pattern Depth (mm)
Gray Value
Distance (mm)
Pattern Depth (mm)
b
1 2 3 4 5 6 7
Pattern Depth (mm)
Gray Value
Distance (mm)
Pattern Depth (mm)
c
1 2 3 4 5 6 7
Pattern Depth (mm)
Gray Intensity
Distance (mm)
Pattern Depth (mm)
d
Red
e
Green
f
Blue

Figure S10. Pattern characterization. (a), PA-GelA hydrogel printed with rIgG and bIgG adjacent to each other – *From Figure 4e*. **(b),** PA-GelA hydrogel with complex multi-molecular patterns including concentration gradients being generated from bIgG patterns transitioning into rIgG patterns – *From Figure 4i*. **(c),** PA-GelA hydrogel with complex multi-molecular patterns including concentration gradients within the same pattern line using rIgG and elastin – *From Figure 4f*. **(d-f),** RGD colour deconvolution of (c). The intensity profile of each image (a-c) is plotted on the right column.

Supporting Section 9. **Materials and methods.**

Numerical Simulations: Numerical simulations of the movement of patterning molecules through a hydrogel at various levels of mask permeability to the solution were performed using the commercial finite element modelling program COMSOL Multiphysics (COMSOL, Sweden).

Cell Culture: Prior to cell inoculation, the printed hydrogels were thoroughly washed with PBS for 20 min and repeated 8 times in order to ensure that the Tris-HCl buffer, TEMED, and uncrosslinked acrylamide were was completely removed. Sterilization was performed by immersing the hydrogel in a 2% solution of penicillin/streptomycin (Sigma-Aldrich, Spain) for 2 h, and washed 5 times for 20 min in PBS to remove the remaining Tris-HCl and penicillin/streptomycin from the sterilizing process. NIH-3T3 cells were expanded in Dulbecco's modified Eagle's medium (DMEM; Life Technologies, Spain) supplemented with 10% fetal bovine serum (FBS; Attendbio Research, Spain), 1% glutamine (Sigma-Aldrich, Spain) and 1% penicillin/streptomycin (Sigma-Aldrich, Spain). Cells were used at

passage 15-18. After harvesting using trypsin-EDTA, the cells were diluted in serum-free DMEM and 2.5×10^5 were seeded onto the top of a 5 mm long slice of the printed hydrogel held in place using the FBC. After 4 h, the non-adhered cells were removed by washing gently with PBS and exchanging the media with fresh DMEM supplemented with 10% FBS. After 24 h of cell inoculation, the hydrogel was transferred to a 24 well plate to allow adequate oxygen and nutrient diffusion. On day 14, cells were fixed with 4% (wv^{-1}) paraformaldehyde (Sigma-Aldrich, Spain) in PBS at 21 °C for 45 min and stained.

Cell Visualization: Initial cell attachment to the hydrogel surface was assessed using a Nikon Eclipse TE200 phase contrast microscope (Nikon Instruments, Japan). For visualization of cell penetration into the hydrogel on day 14, the cells were permeabilized with 0.1% Triton X-100 (Sigma-Aldrich, Spain) for 10 min. In order to observe the actin cytoskeleton, the cells were stained with phalloidin–fluorescein isothiocyanate (phalloidin–FITC) (Sigma-Aldrich, Spain) at a 1:500 dilution in PBS for 60 min at room temperature. The cells were counterstained with the nuclear staining 4′,6-diamidino-2-phenylindole dihydrochloride (DAPI; Life Technologies, Spain). Finally, the hydrogel was positioned cell-side down onto a glass microscope slide. The cells were visualized using a Leica TCS-SP5 confocal microscope (Leica Microsystems, Germany) and the 3D reconstructions were performed using ImageJ Software (NIH, USA).

Supporting Section 10. References

[1] Spectra/Por®, Standard Grade Regenerated Cellulose Dialysis Membrane, Product information & Operating Instructions.